JVI Journals.ASM.org

A Mutation in the Ebola Virus Envelope Glycoprotein Restricts Viral Entry in a Host Species- and Cell-Type-Specific Manner

Osvaldo Martinez,[a] Esther Ndungo,[b] Lee Tantral,[a] Emily Happy Miller,[b] Lawrence W. Leung,[a] Kartik Chandran,[b] Christopher F. Basler[a]

Icahn School of Medicine at Mount Sinai, New York, New York, USA[a]; Department of Microbiology and Immunology, Albert Einstein College of Medicine, Bronx, New York, USA[b]

Zaire Ebola virus (EBOV) is a zoonotic pathogen that causes severe hemorrhagic fever in humans. A single viral glycoprotein (GP) mediates viral attachment and entry. Here, virus-like particle (VLP)-based entry assays demonstrate that a GP mutant, GP-F88A, which is defective for entry into a variety of human cell types, including antigen-presenting cells (APCs), such as macrophages and dendritic cells, can mediate viral entry into mouse CD11b$^+$ APCs. Like that of wild-type GP (GP-wt), GP-F88A-mediated entry occurs via a macropinocytosis-related pathway and requires endosomal cysteine proteases and an intact fusion peptide. Several additional hydrophobic residues lie in close proximity to GP-F88, including L111, I113, L122, and F225. GP mutants in which these residues are mutated to alanine displayed preferential and often impaired entry into several cell types, although not in a species-specific manner. Niemann-Pick C1 (NPC1) protein is an essential filovirus receptor that binds directly to GP. Overexpression of NPC1 was recently demonstrated to rescue GP-F88A-mediated entry. A quantitative enzyme-linked immunosorbent assay (ELISA) demonstrated that while the F88A mutation impairs GP binding to human NPC1 by 10-fold, it has little impact on GP binding to mouse NPC1. Interestingly, not all mouse macrophage cell lines permit GP-F88A entry. The IC-21 cell line was permissive, whereas RAW 264.7 cells were not. Quantitative reverse transcription (RT)-PCR assays demonstrate higher NPC1 levels in GP-F88A permissive IC-21 cells and mouse peritoneal macrophages than in RAW 264.7 cells. Cumulatively, these studies suggest an important role for NPC1 in the differential entry of GP-F88A into mouse versus human APCs.

Zaire Ebola virus (EBOV) is an emerging zoonotic pathogen that causes hemorrhagic fever in humans. Fatality rates in some human outbreaks have approached 90% (reviewed in reference 1). Because of its lethality, the lack of FDA-approved therapeutics, and its potential use as a bioweapon, EBOV is classified as a category A pathogen (2) and is studied under biosafety level 4 containment.

Although wild-type EBOV is highly lethal in nonhuman primate models of infection, it is not lethal in experimentally infected mice or guinea pigs (3, 4). Instead, lethal EBOV infection requires either adaptation of the virus to these species or infection of animals with defects in their antiviral immune responses (3, 5–7). Even after mouse adaptation, EBOV virulence depends upon the route of administration, as intraperitoneal inoculation results in lethal infection, whereas several other routes are not lethal (3). Understanding the molecular basis for host- and tissue-specific restrictions to disease may suggest novel therapeutic strategies. It may also suggest strategies to engineer recombinant EBOVs that are replication competent but attenuated in humans; such viruses could serve as useful scientific tools while posing reduced risk to researchers.

One potential determinant of EBOV tissue tropism and host cell range is viral entry, which is mediated by the EBOV attachment and fusion surface glycoprotein (GP) (8). GP is a type I transmembrane protein cleaved by furin proteases into GP1 and GP2 subunits (9–12). The N-terminal region of GP1 (residues 57 to 149) has been defined as a receptor-binding domain (RBD) (13–16), while GP2 contains the hydrophobic fusion peptide and heptad repeats that mediate membrane fusion (17–19). The bulky C-terminal mucin-like domain in GP1 is extensively modified with O-linked glycans and is not required for viral entry (13, 20). Several potential host cell surface molecules have been shown to enhance EBOV entry into target cells and may serve as attachment receptors, although no single essential cell surface attachment receptor has been identified (21–27). Following attachment to host cells, EBOV particles undergo endocytosis (8), likely through macropinocytosis, although additional endocytic pathways have been implicated (28–34). The internalized virus localizes to acidified endosomes containing the activated cysteine proteases cathepsins L (Cat L) and B (Cat B) (13, 30, 35). These enzymes cleave GP, removing the mucin-like domain and other C-terminal GP1 sequences, generating a primed species competent for entry (13, 16, 30, 35, 36). Niemann-Pick C1 (NPC1), a protein involved in cholesterol transport and storage, serves as an essential intracellular entry receptor (37, 38). Processing of GP by endosomal cysteine proteases uncovers the RBD within the N-terminal region of EBOV GP1, allowing GP to directly bind NPC1, and this interaction requires the C domain of NPC1 (39, 40). For completion of the entry process, additional downstream events are also required (13, 15, 16, 30, 40), including fusion of viral and cellular membranes, in which a hydrophobic fusion loop located at residues 524 to 539 within GP2 plays a crucial role (17).

In this study, we surveyed mouse peritoneal cells (PECs) to identify cell types permissive for EBOV entry in an effort to better understand why intraperitoneal inoculation of mouse-adapted EBOV results in lethal infection (3). Using β-lactamase-tagged EBOV virus-like particles (VLPs) (41, 42), we identified CD11b$^+$

Received 26 June 2012 Accepted 27 December 2012
Published ahead of print 9 January 2013
Address correspondence to Christopher F. Basler, chris.basler@mssm.edu, or Osvaldo Martinez, osvaldo.martinez@mssm.edu.

doi:10.1128/JVI.01598-12

myeloid cells, a population that includes macrophages, as permissive. Strikingly, EBOV VLPs bearing an F88A mutant GP (GP-F88A), previously described as unable to mediate entry into SNB-19 (43), HeLa (31), Vero (30, 41), and 293T (43) cells and human dendritic cells (DCs) (41), could enter mouse peritoneal macrophages and bone-marrow-derived dendritic-cell antigen-presenting cells (APCs) using a pathway similar to that used by wild-type GP (GP-wt) to enter human cells. Mutating other hydrophobic residues, which lie in close proximity to F88, also impaired entry, but not in a mouse APC-specific manner. Because NPC1 is essential for EBOV entry and overexpression of NPC1 rescues GP entry mutants with reduced NPC1 binding (40), we tested whether mouse or human NPC1 domain C bound to GP-wt and GP-F88A differentially. We confirmed that GP-F88A bound poorly to the human NPC1 domain C relative to GP-wt, whereas GP-F88A and GP-wt exhibit more modest differences in binding to mouse NPC1 domain C. By surveying entry into different mouse cell lines, we further correlate permissiveness for GP-F88A with high levels of NPC1 expression. Altogether, the data provide evidence that genetic changes in EBOV GP can modulate the virus host cell range and that this reflects both the relative affinity of GP for NPC1 and NPC1 expression levels.

MATERIALS AND METHODS

Cell lines, plasmids, and antibodies. 293T human embryonic kidney cells; the human hepatoma cell line Huh7; HeLa cells; the guinea pig colonic adenocarcinoma cell line GPc16; and Vero 76, Vero E6, and mouse NIH 3T3 cells were grown in Dulbecco's modified Eagle's medium (DMEM) (Invitrogen, Carlsbad, CA) supplemented with 10% fetal calf serum (Invitrogen), 2 mM L-glutamine (Invitrogen), 100 units/ml of penicillin, 100 μg/ml streptomycin at 37°C in 7% CO_2. The mouse macrophage cell lines RAW 264.7, H36.12a (ATCC CRL-2445), J774, and IC-21 (ATCC TIB-186) were grown in RPMI supplemented with 10% fetal calf serum (Invitrogen), 2 mM L-glutamine (Invitrogen), 100 units/ml of penicillin, 100 μg/ml streptomycin at 37°C in 7% CO_2. The anti-β-lactamase antibody AB3738 was purchased from Chemicon International. EBOV GP was detected using 9c11 (44), a mouse monoclonal anti-EBOV (α-EBOV) mucin domain antibody, or a rabbit polyclonal antibody targeted to the N terminus of EBOV GP (41).

Virus-like particle production. To produce VLPs, 293T cells were cotransfected with two expression plasmids using Lipofectamine 2000 (Invitrogen). The plasmids were pCAGGS β-lactamase-VP40 and a pcDNA plasmid expressing wild-type Zaire EBOV strain Mayinga GP (GP-wt), GP-derived mutants, or vesicular stomatitis virus (VSV) glycoprotein (VSV G). Specifically, VLPs were produced by transfecting a total of 18 μg of expression plasmids into 10^7 293T cells in 10-cm plates using Lipofectamine 2000 (Invitrogen) at a 3:4 ratio of DNA to Lipofectamine, as recommended by the manufacturer. The β-lactamase VP40 (lacVP40) expression plasmid was transfected on its own (18 μg) or in combination (12 μg) with plasmids expressing GP-wt or VSV G (6 μg). Seventy-two hours posttransfection, cells and cellular debris were pelleted away from the harvested VLP-containing supernatant by gentle centrifugation at 175 × *g*. Then, VLPs were centrifuged through a sucrose cushion at 25,000 rpm in an SW-28 rotor for 2 h at 4°C and washed in ice-cold NTE buffer (10 mM Tris, pH 7.5, 100 mM NaCl, 1 mM EDTA) by centrifuging at 25,000 rpm for two more hours at 4°C. The resulting pellet was resuspended in 50 to 100 μl of NTE buffer by tapping gently 100 times. VLPs were left on ice until they were used.

Total β-lactamase activity. The β-lactamase activity of purified VLPs was measured using a fluorogenic substrate (Lytic Blazer; Invitrogen, Carlsbad, CA) as recommended by the manufacturer.

VLP entry assays. VLP entry assays were performed as outlined in a previous study (41). Briefly, VLP preparations were normalized based on β-lactamase activity. The β-lactamase equivalents of different VLP preparations were used in each entry assay. VLPs were "spinoculated" onto target cells at 2,000 rpm for 45 min at 4°C before incubation at 37°C in 1% RPMI for 3.5 h. CCF2AM (Invitrogen) substrate was then loaded onto cells for 1 h at room temperature. The entry of VLPs into cells was assayed by flow cytometry. On average, 5,000 cells were sorted per sample for entry assays using cell lines, and on average, approximately 50,000 cells were sorted per sample for entry assays using *ex vivo* peritoneal cells. The cells were first gated for viability using side scatter (SSC) and forward scatter (FSC) properties, where viable cells are gated for relative low SSC values and relative high FSC values. A violet laser from an LSR II (BD Bioscience) was used to excite the CCF2AM substrate, and cells were assayed for green and blue fluorescence. The cells were further gated for viability using retention of CCF2AM substrate fluorescence. Those cells fluorescing blue relative to the control (for example, the no-VLP control) were scored positive for entry. One advantage of the β-lactamase entry system is that scoring entry is dependent on cytosolic penetration without the need for further downstream events required by other pseudotype-based systems. Of note, although the amounts of each VLP were normalized with respect to total β-lactamase activity, the actual number of particles used in each assay was unknown. The error bars in the entry assay histograms represent the standard deviation of the mean of the replicates for that experiment.

VLP binding assays. Equivalent amounts of VLPs were "spinoculated" onto plated human DCs. The VLP-bound cells were then incubated for 1 h at 4°C, washed with ice-cold phosphate-buffered saline, and then analyzed for total β-lactamase activity.

Western blots. β-Lactamase equivalents of purified VLPs were separated by SDS-PAGE, transferred to polyvinylidene difluoride (PVDF) membranes (Roche), blocked in 2% nonfat milk in Tris-buffered saline (TBS) (50 mM Tris, pH 7.5, 100 mM NaCl) for 1 h, probed overnight with appropriate antibodies diluted in 1% nonfat milk in TBS, washed 3 times in TBS-T (TBS plus 0.05% Tween 20) for 5 min/wash, probed with secondary antibody for 1 h, and washed a final 3 times. The Western blots were developed using a Western Lightning ECL kit (Perkin-Elmer, Boston, MA) and Kodak BioMax film (Kodak, Rochester, NY). The relative band density was determined using ImageJ image-processing software (NIH).

Isolation and culture of human dendritic cells and macrophages. Peripheral blood mononuclear cells (PBMCs) were isolated by Ficoll density gradient centrifugation (Histopaque; Sigma-Aldrich, St. Louis, MO) from buffy coats of healthy human donors (New York Blood Center). $CD14^+$ cells were purified using anti-human CD14 antibody-labeled magnetic beads and iron-based Midimacs LS columns (Miltenyi Biotec, Auburn, CA). After elution from the columns, the cells were plated (0.7×10^6 to 1×10^6 cells/ml) in DC medium (RPMI [Invitrogen, Carlsbad, CA] supplemented with 100 units/ml of penicillin, 100 μg/ml streptomycin, 55 μM β-mercaptoethanol) supplemented with 4% human serum AB (GemCell; Gemini Bio-Products, West Sacramento, CA). Immature DCs were differentiated with 500 U/ml human granulocyte-macrophage colony-stimulating factor (GM-CSF) (Peprotech, Rocky Hill, NJ) and 500 U/ml human interleukin-4 (IL-4) (Peprotech) and incubated for 5 to 7 days at 37°C. By day 5, immature DCs expressed surface CD11c and HLA-DR (major histocompatibility complex class II [MHC-II]), but low to no CD14. Macrophages were differentiated with M-CSF (Peprotech) or GM-CSF without IL-4 for at least 7 days.

Preparation of mouse peritoneal cells and bone marrow antigen-presenting cells. Peritoneal cells were harvested from sacrificed C57/BL6 mice. To harvest macrophages (approximately 5% to 15% of the normal peritoneal cell compartment), naive mice were used. Normally, the mouse peritoneum contains few if any granulocytes. To harvest greater numbers of peritoneal macrophages, mice were induced for approximately 4 days with intraperitoneally inoculated 3% thioglycolate solution. To harvest granulocytes and macrophages, the mice were induced overnight or for 24 h with intraperitoneally inoculated 3% thioglycolate solution. Specifi-

cally, to harvest PECs, 2 ml of Hanks' balanced salt solution was introduced through a small abdominal incision into the peritoneum of the mouse, the abdomen was massaged, and the solution containing the PECs was harvested. The PECs were either used immediately or incubated overnight in DMEM (Invitrogen, Carlsbad, CA) supplemented with 10% fetal bovine serum (FBS) (Invitrogen), 2 mM L-glutamine (Invitrogen), 100 units/ml of penicillin, 100 μg/ml streptomycin, with incubation at 37°C in 7% CO_2. EBOV GP-mediated entry efficiency was not affected when PECs were used 1-day postharvesting rather than the same day.

C57/BL6 mouse bone marrow cells were harvested and strained through a 70-μM cell strainer (BD Bioscence) and washed. Specific $CD11b^+$ or $CD34^+$ cells were isolated using beads and columns with products and protocols suggested by the manufacturer (Miltenyi Biotech); otherwise, total bone marrow cells were differentiated. Specific or total cells were resuspended in DMEM (Invitrogen, Carlsbad, CA) supplemented with 10% FBS (Invitrogen), 2 mM L-glutamine (Invitrogen), 100 units/ml of penicillin, 100 μg/ml streptomycin and incubated at 37°C in 7% CO_2. To differentiate bone marrow cells, the medium was supplemented with GM-CSF or M-CSF (20 ng/ml) and replenished every 3 days with 10 ng/ml.

Flow cytometry. Flow cytometry was performed using an LSR II flow cytometer equipped with a violet laser (BD Bioscience). The data were analyzed using Flo Jo software (Tree Star, Ashland, OR).

DC treatments. Day 5 to 7 human DCs were plated in 24-well dishes (0.4×10^6 cells/well) in DC medium supplemented with 1% dimethyl sulfoxide (DMSO) and 2% human serum AB (GemCell) and either mock treated or pretreated with decreasing concentrations of the indicated inhibitor for 2 h prior to infection.

Viral particles containing GP_{CL}. VSV particles containing cleaved GP (GP_{CL}) were generated as described previously (36). Briefly, VSV-GP-EBOV particles were incubated with thermolysin (200 μg/ml) for 1 h at 37°C. The protease was inactivated by addition of phosphoramidon (1 mM), and the reaction mixtures were used immediately.

GP-NPC1 binding ELISA. GP-NPC1 enzyme-linked immunosorbent assays (ELISAs) were performed essentially as described previously (40). Briefly, high-binding ELISA plates (Corning) were coated with the GP-specific monoclonal antibody KZ52 (2 μg/ml in phosphate-buffered saline [PBS]) and then blocked with PBS containing 3% bovine serum albumin (PBSA). *In vitro*-cleaved particles of VSV expressing EBOV GP-wt or GP-F88A that had been solubilized in PBSA buffer were added to the blocked plates, and GP capture was allowed to proceed for 1 h at 37°C. After washing to remove unbound GP, serial dilutions of purified, Flag-tagged mouse or human NPC1 soluble domain C (0 to 1 μg/well) was added to the wells. After incubation at 37°C for 1 h, the plates were extensively washed, and bound Flag-tagged proteins were detected with an anti-Flag antibody-horseradish peroxidase conjugate and Ultra-TMB substrate (Thermo). After background subtraction and data normalization, binding curves were fitted to a logistic equation (Graphpad Prism) to derive the 50% effective concentration (EC_{50}), the NPC1 domain C concentration at which half-maximal binding to GP is obtained. The GP concentrations of different viral preparations were pretitrated for the GP-NPC1 binding assay in a separate GP ELISA, as described previously (40).

Production of VSV pseudotypes and measurement of viral infectivity. VSV pseudotypes bearing filovirus glycoproteins (VSV-GP) were generated as described previously (36, 45). Infectivities of VSV pseudotypes were measured by manual counting of enhanced green fluorescent protein (EGFP)-positive cells using fluorescence microscopy at 16 to 24 h postinfection. Briefly, cell monolayers in 48-well plates were exposed to serial 10-fold dilutions of viral inoculum, and infected cells were enumerated at a viral dilution that yielded 50 to 100 EGFP-positive cells. Cell counts were corrected for viral dilution to generate infectious titers (infectious units [IU]/ml).

Quantitative reverse transcription (qRT)-PCR. qRT-PCR gene amplification was performed using the iQ SYBR green Supermix (Bio-Rad) according to the manufacturer's instructions. The PCR temperature profile was 95°C for 10 min, followed by 40 cycles of 95°C for 10 s and 60°C for 60 s. All the reactions were performed in triplicate, and standard-error bars are indicated on the graphs. A no-reverse-transcriptase control was used to show that the NPC1 expression levels detected were not due to contaminating DNA. CXF Manager software (Bio-Rad) was used to analyze the relative mRNA expression levels by the change in threshold cycle (ΔC_T) method using the β-actin gene to normalize the results. To determine NPC1 mRNA levels in murine cells, murine-specific forward (TCT GAATGCGGTCTCCTTG) and reverse (TATGGCTGCAGAACTCC ACA) primers were used.

RESULTS

Primary mouse, but not human, APCs are permissive for GP-F88A-mediated entry. For the experiments described below, EBOV VLPs were generated by expressing an EBOV VP40 matrix protein fused at its N terminus to β-lactamase, which can function as a reporter for VLP entry (41, 42, 47). This VP40 fusion was coexpressed with either wild-type or mutant EBOV GP or control VSV G, resulting in the incorporation of the glycoproteins, either of which can mediate entry, into the VLPs (41). To assay for successful entry, target cells were first loaded with a membrane-permeable β-lactamase substrate (CCF2AM; Invitrogen), which is cleaved by cytoplasmic esterase to become membrane impermeable. Successful VLP entry results in the delivery of β-lactamase into the cytoplasm, where it cleaves the CCF2AM substrate. Once cleaved by β-lactamase, the substrate fluoresces blue, whereas the uncleaved form fluoresces green (41, 42, 47, 48). Equivalent amounts of VLPs, as determined by assaying the total β-lactamase activity of purified VLP preparations, were used to infect human monocyte-derived DCs or mouse PECs (Fig. 1). After 3.5 h, human DCs infected with GP-wt VLPs were positive for cytoplasmic β-lactamase activity (blue fluorescing). In contrast, GP-F88A VLPs were unable to enter human DCs, consistent with previous reports that the mutant is defective for EBOV entry (Fig. 1A) (43, 49). Furthermore, entry assays using human DCs derived from monocytes isolated from different donors consistently (experiments were repeated 6 times) resulted in significant entry by GP-wt (entry into as many as 90% of all cells), while entry by GP-F88A never rose above 10% (Fig. 1 and data not shown; see Fig. 4 and 5C and D). In addition, prestimulation of the cells with Toll-like receptor 2 (TLR2) and -4 agonists, which is expected to increase antigen uptake, also failed to enhance entry into the human DCs (data not shown).

Strikingly, a subpopulation of mouse PECs could be infected by VLPs possessing either GP-wt or GP-F88A, a mutant previously demonstrated to be entry defective in a number of cell types (Fig. 1B). This experiment was repeated with similar results over 10 times. Entry by GP-wt and GP-F88A VLPs was inhibited by the pancysteine protease inhibitor E64d (Fig. 1B), indicating that entry into the mouse cells by both GPs is cysteine protease dependent, as previously described for EBOV GP-mediated entry into a variety of cells (13, 16, 20, 30, 35, 36, 41, 43, 49, 50). In contrast, and as expected, VLPs possessing VSV G entered PECs efficiently in a cysteine protease-independent manner, demonstrating the specificity of the inhibitor in this entry assay (Fig. 1B).

PECs consist of a mixed population of mostly B lymphocytes, T lymphocytes, and macrophages. In the analysis of Fig. 1B, after gating on live peritoneal macrophages and lymphocytes (14,390 cells), cells were analyzed for entry using GP-F88A VLPs (no treatment), and the percentage of cells that were entry positive was shown to be 2.81% (404 cells out of 14,390 total cells). To deter-

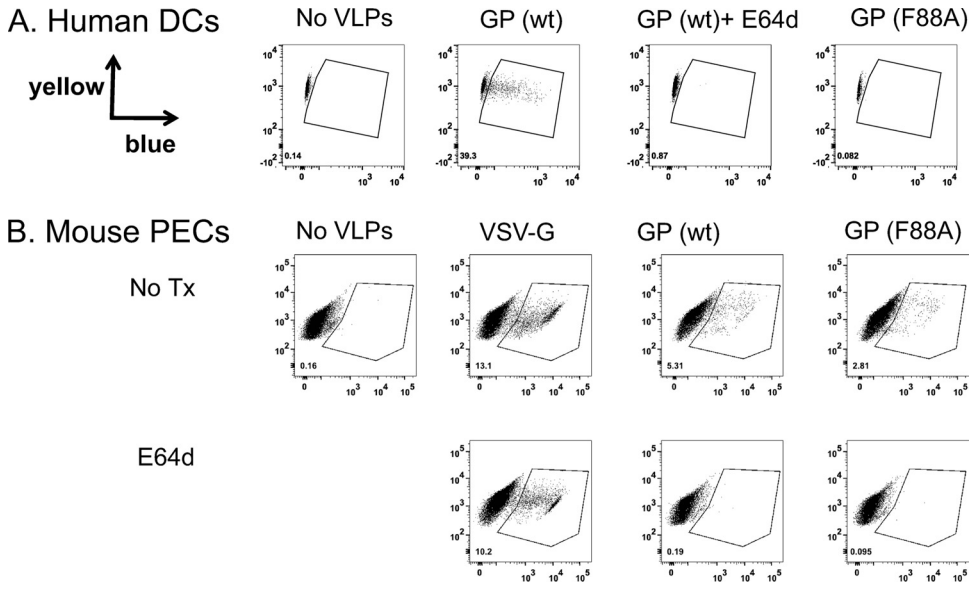

FIG 1 GP-F88A is permissive for entry into mouse peritoneal cells, but not human dendritic cells. Equivalent amounts of VLPs, as determined by assaying the total β-lactamase activity of purified VLP preparations possessing wt GP [GP (wt)], GP-F88A [GP (F88A)], or VSV G were used to infect human monocyte-derived DCs (A) or mouse PECs (B). Mock-infected cells (No VLPs) served as a control. +E64D indicates infections performed in the presence of the pancathepsin inhibitor e64d. The gates indicate entry-positive cells; the percentage of entry-positive cells is indicated by the number in the lower left of each panel. Entry assays demonstrating the GP-F88A entry defect in human DCs were repeated with similar results in 6 independent experiments. Entry assays demonstrating GP-F88A-mediated entry into PECs were repeated 10 times with similar results. No Tx, no transfection.

mine what cell types within the PEC population were infected by GP-wt and GP-F88A VLPs, an entry assay was performed, and cells were gated by using flow cytometer FSC and SSC parameters, crude measures of size and granularity, respectively. Entry-positive cells were relatively large (data not shown), suggesting that they were macrophages and not lymphocytes. The experiment was repeated, but PECs were stained with representative stains for T lymphocytes (anti-CD3) and myeloid cells, including macrophages (anti-CD11b) (Fig. 2A). Gating on the β-lactamase-positive cells demonstrated that both GP-wt and GP-F88A VLPs infected $CD11b^+$ PECs (Fig. 2A), but not $CD3^+$ T lymphocytes (data not shown), consistent with previous reports that lymphocytes, including T lymphocytes, are resistant to EBOV infection (51, 52). The $CD11b^+$ PECs also stained positive for the macrophage/monocyte marker $F4/80^+$ (data not shown) and are therefore likely to be macrophages. Peritoneal macrophages (PEMs) are professional phagocytes, well known for their ability to ingest a multitude of antigens. To address the possibility that the VLP entry into PEMs occurs by a nonspecific, surface glycoprotein-independent mechanism, infection by VLPs lacking a surface viral glycoprotein was compared with infection by the VSV G, GP-wt, and GP-F88A VLPs (Fig. 2B). We also tested whether another mouse APC, bone marrow-derived dendritic cells (BM-DCs), was entered by any of these VLPs. Entry was shown to be dependent on the presence of a viral glycoprotein, as purified β-lactamase equivalents of VLPs made by expressing β-lactamase-VP40 in the absence of a viral glycoprotein did not enter any cell tested (Fig. 2B). Further, mouse PEMs, as well as BM-DCs, were entered by VSV G, GP-wt, and GP-F88A VLPs.

Although, all infected PECs were $CD11b^+$ (PEMs) (Fig. 2A), not all PEMs were infected in these experiments (Fig. 1 and 2A). To determine the relative efficiency with which GP-wt versus GP-F88A VLPs infect PEMs and whether all PEMs are permissive for EBOV entry, increasing concentrations of GP-wt and GP-F88A VLPs were used to infect PEMs. The entry of GP-wt was more efficient; for example, 50% PEM infection required approximately 3 times more β-lactamase equivalents of GP-F88A VLPs than GP-wt VLPs (not shown and Fig. 2C). Despite this difference, increasing PEM infection occurred with increasing concentrations of either GP-wt or GP-F88A VLPs, and each preparation plateaued with approximately 90% of cells infected (Fig. 2C). These data demonstrate that the large majority of PEMs are permissive for both GP-wt- and GP-F88A-mediated entry. In contrast, although increasing amounts of the GP-wt VLPs led to increasing infection of Vero cells, plateauing at 60%, no entry into Vero cells was detected at any of the tested concentrations of GP-F88A VLPs (Fig. 2D).

Identification of hydrophobic residues in proximity to F88 required for efficient entry into mouse and human APCs. The structure of EBOV GP shows that residue 88 of Zaire EBOV GP is partly exposed at the surface of the GP and is adjacent to hydrophobic amino acid residues L111, I113, L122, and F225, the last of which is predicted not to be present in the protease-cleaved GP (GP_{CL}) (Fig. 3) (53). We asked whether mutating the other residues to alanine would reveal entry phenotypes similar to that of GP-F88A in human cells, murine cells, or other cell types potentially relevant to EBOV infection. Equivalent amounts, based on β-lactamase activity, of GP-wt, GP-F88A, GP-L111A, GP-I113A, GP-L122A, and GP-F225A VLPs were generated and used in entry assays. GP-F159A VLPs were also generated, because residue 159 does not localize near F88 and because the F159A mutation has previously been demonstrated to abrogate entry into a variety of cell types (43, 49, 54). VLP entry assays were performed on human DCs; human macrophages; the human cell lines HeLa, HEK293T, and Huh7, each of which is permissive for EBOV infection (27, 29, 31, 41, 55, 56); the nonhuman primate Vero cell line; primary

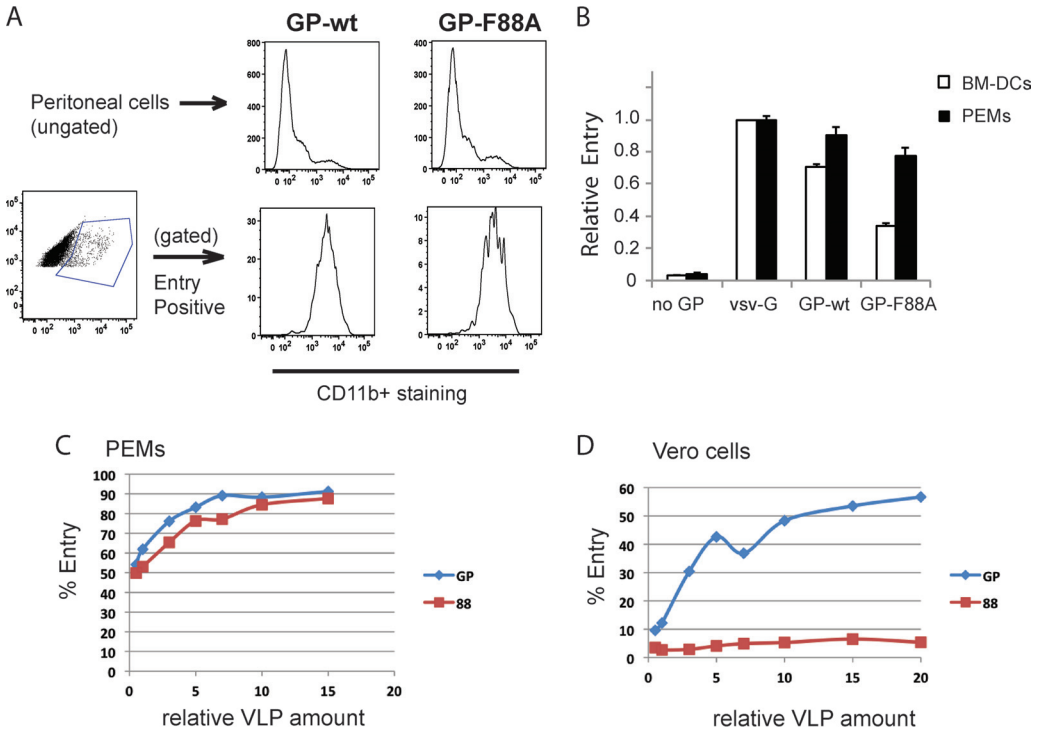

FIG 2 GP-wt and GP-F88A mediate entry into mouse antigen-presenting cells. (A) To determine what cell types within the PEC population were infected by GP-wt and GP-F88A VLPs, peritoneal cells were stained with anti-CD3 and anti-CD11b antibodies. Gating on the β-lactamase-positive cells determined that both wt GP and GP-F88A VLPs infected $CD11b^+$ cells. (B) Equivalent amounts, based on β-lactamase activity, of VLPs containing no viral attachment glycoprotein (lacVP40), VSV-G (lacVP40 plus VSV-G), wild-type GP (lacVP40 plus GP), or GP-F88A (lacVP40 plus GP-F88A) were used to infect mouse PEMs and mouse BM-DCs. The *y* axis indicates relative entry into cells. (C and D) Increasing concentrations of GP-wt (GP) and GP-F88A (88) VLPs were used to infect PEMs (C) and Vero 76 cells (D). For these comparisons, VLPs were adjusted to equal infectivity, based on entry assays performed on PEMs. Since entry by GP-wt VLPs was more efficient than that by GP-F88A VLPs, ~3-fold more β-lactamase units of GP-F88A VLPs than GP-wt VLPs were used in order to start the titration. Each point in panels C and D represents a single entry assay. The experiments shown in panels C and D were repeated with similar results.

murine DCs; and the guinea pig cell line GPc16. Shown in Fig. 4A are the levels of entry by VLPs prepared with different GP mutants, presented as a percentage of entry by GP-wt for that particular cell type. Accompanying Fig. 4 is Table 1, which provides entry data for GP-wt and GP-F88A entry into the cell types shown in Fig. 4. In Table 1, the average percent entry into each cell type is provided, along with GP-F88A/GP-wt entry ratios. GP-F88A displayed reduced entry, relative to GP-wt, into mouse BM-DCs, consistent with our prior data. GP-F88A also entered the guinea pig GPc16 cells, albeit inefficiently. Weak GP-L111A entry was seen in murine DCs, human DCs, and Vero cells, while no entry was noted in other cells. Yields of GP-I113A VLPs were consistently low, making it difficult to isolate amounts sufficient to test all cells for entry (data not shown). Of the cells tested, GP-I113A VLPs could modestly infect human and mouse DCs and inefficiently entered HeLa and Huh7 cells. GP-L122A VLPs infected mouse DCs, as well as Vero and GPc16 cells, with modest efficiency. It is notable that this mutant, despite infecting Vero cells, displayed no significant entry into the human cells tested. As expected, the GP-F159A mutant failed to enter any of the cell types (43, 49, 54). In contrast to the other mutants, GP-F225A VLP entry was as efficient as wild-type GP or, in the case of GPc16 and Vero cells, more efficient than wild-type GP entry. These data demonstrate a critical role for all of the F88-proximal residues, with the exception of F225, in EBOV entry. The data also demonstrate that individual mutants exhibit different efficiencies of entry into different cell types. However, only the F88A mutant exhibits a tropism for murine APCs.

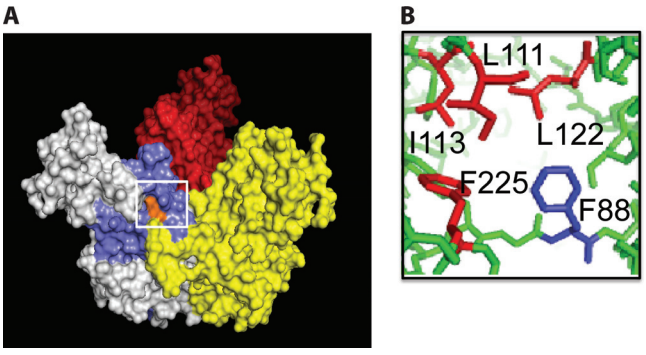

FIG 3 Location of GP residue F88. (A) The EBOV GP trimeric ectodomain lacking the GP mucin domain, with the monomers colored white, red, and yellow. The membrane-proximal portion of GP is at the bottom. The N-terminal region of the ectodomain (colored blue) is thought to play a role in receptor binding. (B) Residue 88 of Zaire EBOV GP is partly exposed at the surface of the GP (residue F88 is shown in orange in panel A) and is located near several other hydrophobic residues, including L111, I113, L122, and F225.

The level of incorporation of each mutated GP within each VLP preparation was compared to that of GP-wt. Western blots for each of the purified VLP preparations were probed with anti-β-lactamase and anti-GP antibodies. Shown in Fig. 4B are the

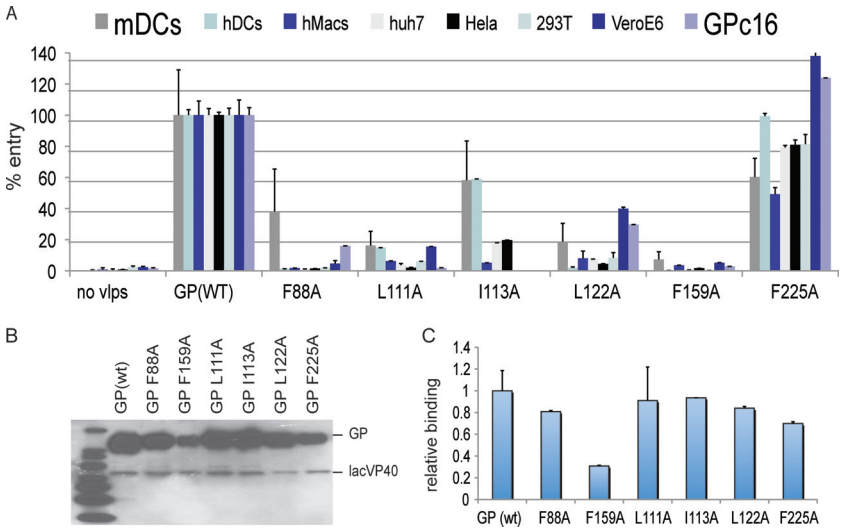

FIG 4 Impacts of mutations to hydrophobic residues near F88 on entry into different cell types. (A) Equivalent amounts, based on β-lactamase activity, of GP-wt, GP-F88A, GP-L111A, GP-I113A, GP-L122A, GP-F159A, and GP-F225A VLPs were generated and tested in entry assays. As a negative control, GP-F159A VLPs were also generated. VLP-mediated infection was performed on human DCs (hDCs); human macrophages (hMacs); the human cell lines HeLa, HEK293T, and Huh7, each of which is infectible with Zaire EBOV; the nonhuman primate Vero cell line; primary murine bone marrow-derived DCs (mDCs); and the guinea pig cell line GPc16. The *y* axis indicates the entry for each VLP as a percentage of the entry of GP-wt for that particular cell type. GP-I113A VLP entry into 293T, Vero, and GPc16 cells was not tested. (B) Western blots of each purified VLP used in panel A were developed with anti-β-lactamase and anti-GP antibodies, demonstrating the relative levels of lacVP40 and GP in each VLP preparation. (C) Relative binding of each VLP preparation to human DCs. The error bars indicate standard deviations of the mean.

relative levels of lacVP40 and GP in the preparations of lacVP40 plus GP, lacVP40 plus GP-F88A, lacVP40 plus GP-L111A, lacVP40 plus GP-I113A, lacVP40 plus GPL122A, lacVP40 plus GP-F159A, and lacVP40 plus GP-F225A VLPs. Only modest differences in the levels of GP-F88A, GP-L111A, GP-I113A, and GP-L122A incorporation into lacVP40 VLPs, compared to GP-wt, were noted. However, there was a significantly lower level of GP-F159A and GP-F225A than of GP-wt incorporated into the lacVP40 VLPs.

To determine whether the F88-proximal mutants exhibit altered binding to the surfaces of human DCs, VLPs were added to DCs at 4°C and washed; binding was then assessed by quantifying cell-associated β-lactamase activity. As shown in Fig. 4C, with the sole exception of GP-F159A, human DCs demonstrated similar levels of binding to each of the different VLPs, suggesting that defects in entry for these mutants are not due to loss of cell surface binding activity.

GP-F88A entry into mouse APCs occurs via macropinocytosis and requires an intact fusion peptide. The cathepsin dependence of GP-F88A entry into mouse APCs is consistent with its use of the canonical filoviral entry pathway. To examine another aspect of the entry pathway, the sensitivity of entry by GP-wt and GP-F88A into PEMs to EIPA [5-(*N*-ethyl-*N*-isopropyl)], an amiloride inhibitor of the Na^+/H^+ exchanger that blocks macropinocytosis (57) and inhibits filovirus entry (29, 33), was assessed. As demonstrated in Fig. 5A, both GP-wt and GP-F88A VLPs were sensitive to EIPA. Inhibition was seen at concentrations at which VSV G-dependent entry, which does not require macropinocytosis, was intact. Only at higher concentrations of EIPA was VSV G-mediated entry inhibited, suggesting nonspecific effects of the compound. These data are consistent with a model in which both GP-wt and GP-F88A enter PEMs via macropinocytosis.

We next checked whether mutation of putative fusion peptide residue F535, a mutation that was previously shown to block GP-mediated entry (F535R), by itself or in combination with F88A could also block entry into PEMs and human DCs. Figure 5 shows that mutating GP residue 535, whether by itself or in combination with F88A, ablated entry into PEMs (Fig. 5B) and into human monocyte-derived DCs isolated from two different subjects (Fig. 5C and D), demonstrating that EBOV GP-mediated entry into PEMs, like entry into other cell types, requires the viral fusion machinery (17).

Differential effects of the GP-F88A mutation on interaction with human versus mouse NPC1 domain C. Overexpression of NPC1 was recently demonstrated to rescue entry of GP-F88A (40). Furthermore, NPC1 domain C is sufficient to interact with GP provided GP is first cleaved by cysteine cathepsins or thermolysin to generate GP_{CL} (40). To address GP-NPC1 interaction, an established ELISA was used to measure the capacities of precleaved GP-wt (GP_{CL}-wt) and GP-F88A (GP_{CL}-F88A) to bind to purified, soluble NPC1 domain C proteins. GP_{CL}-F88A displayed

TABLE 1 Efficiency of GP-wt and GP-F88A entry into cells shown in Fig. 4A

Cell type	% Cell entry		Relative entry (GP-F88A/GP-wt)
	GP-wt	GP-F88A	
Murine DCs	24.15	9	0.37
Human DCs	66.85	0.879	0.01
Human macrophages	43.9	0.758	0.02
HUH7	52.15	0.625	0.01
HeLa	27.55	0.393	0.01
293T	47.6	0.879	0.02
VeroE6	55.95	2.605	0.05
GPc16	44.7	7.16	0.16

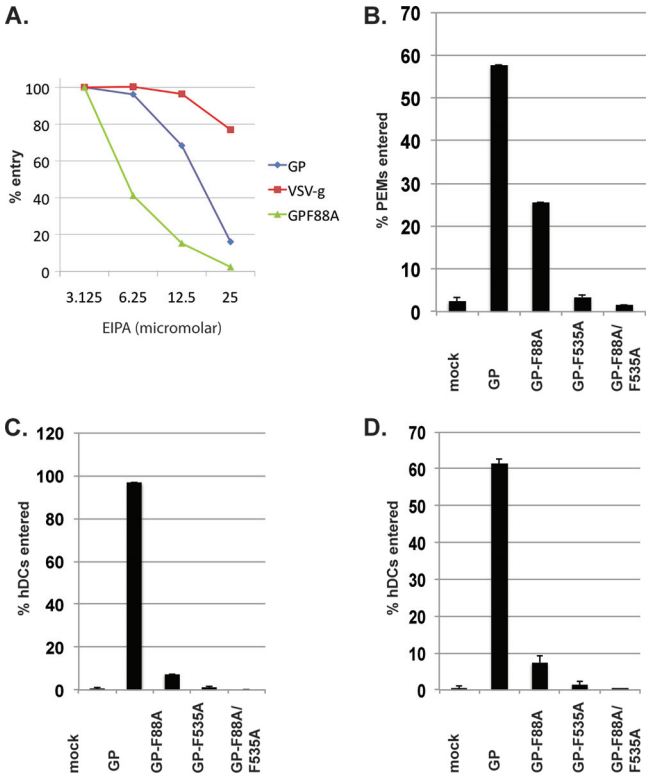

FIG 5 F88A entry into mouse PEMs occurs via macropinocytosis and requires an intact fusion peptide. (A) PEMs were preincubated for 30 min with 2-fold dilutions of EIPA, an amiloride inhibitor of the Na^+/H exchanger. Shown is relative VLP entry of equivalent amounts, based on β-lactamase activity, of GP-wt, GP-F88A, and control VSV G VLPs into PEMs in the presence of inhibitor. Each point on the graphs represents a single entry assay. The experiment was repeated with similar results. (B to D) β-Lactamase equivalents of GP-wt, GP-F88A, the fusion peptide mutant GP-F535R, and the combination GP-F88A and fusion peptide mutant (GP-F88A/GP-F535R) VLPs were tested for entry into PEMs (B) and human DCs generated from monocytes isolated from two different individuals (C and D). The error bars indicate standard errors.

moderately reduced binding to human NPC1 domain C relative to GP_{CL}-wt ($EC_{50\ F88A}/EC_{50\ wt}$, ~10) (Fig. 6). In contrast, while both GP_{CL}-wt and GP_{CL}-F88A bound less efficiently to mouse NPC1 domain C than to the human protein, the F88A mutation had only a modest impact on GP-NPC1 binding ($EC_{50\ F88A}/EC_{50\ wt}$, ~2) (Fig. 6). EC_{50} values for GP_{CL}-wt and GP_{CL}-F88A binding to mouse and human NPC1 domain C are provided in Table 2. These findings are consistent with a model in which GP_{CL}-F88A remains permissive for entry into mouse APCs because its interaction with mouse NPC1 is of sufficiently high affinity.

TABLE 2 Capacities of cleaved GP-wt and GP-F88A proteins to bind to human and murine NPC1 domain C

Cleaved VSV-GP	NPC1 domain C	GP-domain C binding EC_{50} (nM)[a]
GP-wt	Human	0.4 ± 0.1
	Murine	2 ± 1
GP-F88A	Human	5 ± 1
	Murine	3 ± 2

[a] ±Standard deviations from at least three experiments.

Mouse macrophage IC-21 cells are susceptible to entry with GP-F88A VLPs and permit infection with GP-F88A-pseudotyped VSV. We next examined whether murine cell lines are also permissive for GP-F88A-mediated entry. We compared GP-wt and GP-F88A VLP-mediated entry using murine fibroblast NIH 3T3 cells and murine macrophage J774, RAW 264.7, H36.12a, and IC-21 cell lines. Of these, only the IC-21 cells were permissive for GP-F88A-mediated VLP entry (data not shown). Representative entry assays illustrate GP-wt entry into RAW 264.7 (Fig. 7A) and IC-21 (Fig. 7B) cells and GP-F88A-mediated entry into IC-21 cells. The entry assays performed with RAW cells were repeated more than 6 times, including experiments in which RAW 264.7 cells were pretreated with TLR agonists to stimulate phagocytosis, and consistently demonstrated them to be nonpermissive for GP-F88A-mediated entry (data not shown).

We assessed the relative levels of murine NPC1 by qRT-PCR in NIH 3T3, J774, RAW 264.7, H36.12a, and IC-21 cells and PEMs and found that only IC-21 cells expressed NPC1 mRNA at levels comparable to those in PEMs (Fig. 7C and data not shown).

To determine whether GP-F88A can access an entry pathway that leads to virus replication, VSVs pseudotyped with GP-F88A or GP-wt were tested for efficiency of infection of IC-21 and Vero cells. VSV-GP-wt efficiently infected both Vero (~4×10^8 IU/ml)

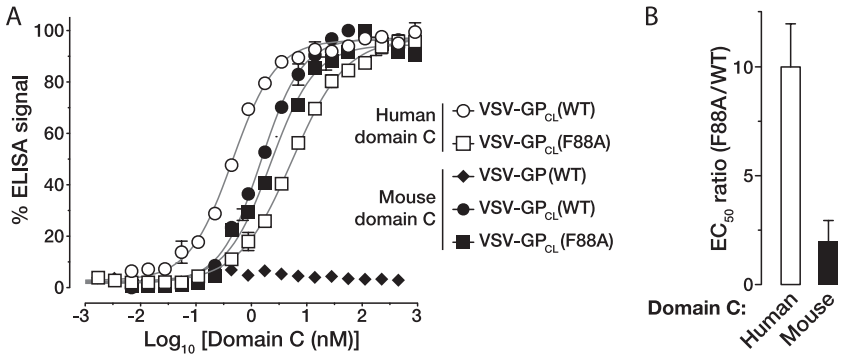

FIG 6 Differential effects of the F88A mutation on interaction of cleaved GP with human versus mouse NPC1 domain C. (A) VSV particles containing uncleaved GP-wt or *in vitro*-cleaved GP_{CL}-wt or GP_{CL}-F88A were captured on ELISA plates coated with the GP-specific monoclonal antibody KZ52. Flag-tagged human or mouse NPC1 soluble domain C was added to the wells, and binding of domain C was detected with an anti-Flag antibody conjugated to horseradish peroxidase. Normalized curves for binding of GP and GP_{CL} to human and mouse domain C are shown. Binding curves were fitted to a logistic equation (the best-fit lines [$r^2 > 0.95$] are shown). (B) Ratios of EC_{50}s (nM domain C) for binding of GP_{CL}-F88A and GP_{CL}-wt to human or mouse NPC1 domain C. The ratios (averages ± standard deviations) represent 4 to 6 trials from at least two independent experiments.

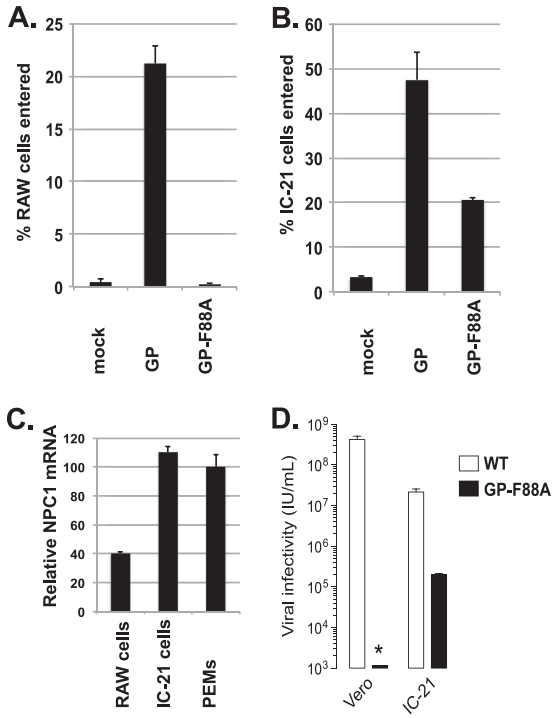

FIG 7 Mouse IC-21 macrophages are susceptible to entry by GP-F88A VLPs and permit infection with GP-F88A-pseudotyped VSV. (A and B) Equivalent amounts, based on β-lactamase activity, of GP-wt and GP-F88A VLPs were tested for entry into RAW cells (A) or IC-21 cells (B). (C) Levels of murine NPC1 mRNA were assayed from RAW and IC-21 cells and PEMs using qRT-PCR normalized to beta actin. (D) Vero and IC-21 cell monolayers were exposed to VSV particles pseudotyped with GP (WT) or GP(F88A). After 16 h at 37°C, infection was scored by manual counting of EGFP-positive cells. The asterisk denotes the limit of detection in the experiment. The error bars indicate standard errors.

and IC-21 (~2×10^7 IU/ml) cells, but VSV-GP-F88A infected only IC-21 cells (Fig. 7D), albeit at significantly lower levels (~2×10^5 IU/ml) than GP-wt (~2×10^7 IU/ml).

DISCUSSION

EBOVs are zoonotic pathogens that cause severe disease in humans and nonhuman primates but do not cause disease in wild-type mice or guinea pigs unless first adapted to these species. The peritoneal route of infection is lethal in the mouse model following infection with a mouse-adapted EBOV, whereas inoculation via the subcutaneous, intradermal, or intramuscular route was not (3, 58). We found that the vast majority of PECs permissive for entry are PEMs, and we further showed that mouse myeloid DCs were also permissive for infection (Fig. 2). It has been proposed that EBOV targets APCs, such as macrophages, for infection and that their infection contributes to the manifestations of EBOV hemorrhagic fever (3–7, 52, 58–62). Therefore, defining intermolecular interactions that influence the outcome of APC infection has relevance to EBOV pathogenesis.

The same mouse APCs permissive for GP-wt entry are also permissive for entry by GP-F88A, despite the fact that this mutant has repeatedly been found to be profoundly defective for entry into a variety of cells, including 293T, SNB-19, Vero, and HeLa cells (Fig. 1 and 4) (43, 49, 54, 63).

The basis for GP-F88A restriction in primate cells remains incompletely defined. Based on the available X-ray crystal structure of the ectodomain of a GP with the mucin-like domain deleted, GP-F88 is located in a hydrophobic area that is partially exposed to the surface (15, 53). GP-F88 lies between the putative RBD (Fig. 3A) and an internal loop thought to be important for the fusion function of the GP. It has been proposed that the GP-F88A mutation might affect either GP binding or the GP fusion event (15).

Several studies have attempted to shed light on the mechanism behind the GP-F88A entry defect by characterizing several parameters that may affect entry, including the efficiency of GP-F88A virion incorporation, the efficiency of GP-F88A processing by cathepsin or thermolysin, and the efficiency of binding to target cells. Our study demonstrated only a modest decrease in the incorporation of GP-F88A into our VLPs compared to wild-type GP (Fig. 4B), consistent with prior reports (41, 43, 49, 63). Further, GP-F88A has been demonstrated to be susceptible to both thermolysin (49) and cathepsin B or L cleavage (43), similar to wild-type GP. This suggests that the defect in GP-F88A entry into primate cells is not at the level of VLP incorporation or GP processing.

Two previous studies suggest that the inability of GP-F88A to mediate entry is at least partly due to a defect in cell binding. Studies by Ou et al. (49), which used murine leukemia virus-pseudotyped GP-(F88A/wt), and Brindley et al. (43), which used pseudotyped feline immunodeficiency virus, showed 40% of GP-wt binding to Vero cells and weak competition by GP-F88A versus GP-wt in binding of virions to SNB-19 cells, respectively. In our study, GP-F88A and mutants of other residues near residue F88 were found to bind with similar efficiencies to human DCs. It should be noted that APCs, such as human DCs, express high levels of surface lectins that can bind GP (21, 22, 25, 64–73) and presumably enhance EBOV infection (27). Therefore, the similar binding demonstrated for GP-F88A VLPs, as well as mutant GP-L111A, GP-I113A, GP-L122A, and GP-F225A VLPs, may be a consequence of the ability of DCs to bind EBOV GP using a variety of cell surface attachment proteins. We speculate that the poor binding of GP-F159A VLPs to DCs may be due to a combination of poor GP incorporation into VLPs (Fig. 4) and altered GP conformation, as evidenced by its inability to be cleaved by thermolysin (49). Although we cannot rule out the possibility that this entry defect in human DCs is related to poor binding to a surface receptor(s), APCs function to sample the environment and feature sustained macropinocytosis. This allows APCs to constantly bind and endocytose environmental antigens, including viruses.

The phenotype of the GP-F88A mutant differs from that displayed by mutants at the other nearby hydrophobic residues, L111, I113, L122, and F225 (Fig. 3). Mutating residue F225 to an alanine modestly enhanced or decreased the efficiency of entry into a variety of cell types, but this mutation did not abrogate entry (Fig. 4). Mutating residues L111, I113, and L122 to alanine significantly decreased the efficiency of VLP entry into several cell types, but not in a species-specific manner. The different mutated GPs were incorporated to similar levels into purified VLPs (Fig. 4B), with the exception of the F225 and F159 mutations, which were incorporated to a lesser extent. Based on these data, the levels of GP incorporation cannot explain the difference in entry between the different VLPs. Therefore, the reason that these mutants behave differently than GP-F88A remains unclear; however, the data

do suggest residues F88, L111, I113, and L122 play an important role in entry and that their locations in the GP are potential antiviral targets.

In several respects, GP-F88A-mediated entry into mouse PEMs resembles GP-wt entry into either mouse or human cells. Studies using virus particles pseudotyped with EBOV GP or live EBOV, and also using chemical inhibitors of clathrin- and caveola-mediated endocytosis, suggest the use of caveolae and/or clathrin in EBOV entry (28, 31, 74). However, cells that lack caveolae can still be infected with EBOV (47), and recent studies support macropinocytosis, a process that can lead to the uptake of large particles, as important for EBOV entry (28–34). Once EBOV particles are internalized and localized to acidified endosomes, activated Cat L and Cat B (13, 30, 35) are required for GP processing. We found that GP-F88A- and GP-wt-mediated entry into PEMs can be inhibited by EIPA in a dose-dependent manner (Fig. 5A) and that the process of entry into PEMs is cathepsin dependent, since the pancathepsin inhibitor e64d inhibited EBOV GP- and GP-F88A-mediated, but not VSV-G-mediated, entry (Fig. 1). Furthermore, the GP F535R mutation localized to the putative fusion peptide of EBOV GP ablated entry into PEMs (Fig. 5B), suggesting that EBOV VLP entry into PEMs also requires GP-mediated membrane fusion.

Recent work has shown that GP-F88A is defective for viral entry at least in part because it binds poorly to the full-length human form of the critical filovirus receptor NPC1 (40). Consistent with this hypothesis, overexpression of human NPC1 rescued the ability of GP-F88A to mediate entry into CHO cells, which are normally refractory to GP-F88A-mediated entry (40). Here, we confirm that the F88A mutation reduces, but does not eliminate, binding of GP_{CL} to a purified, soluble form of human NPC1 domain C. Unexpectedly, however, GP_{CL}-wt and GP_{CL}-F88A bound to mouse NPC1 domain C with similar efficiencies. These findings point to differences in the modes of GP-NPC1 interaction between human and mouse NPC1 and suggest that the retention of mouse NPC1 binding to GP_{CL}-F88A contributes to the capacity of GP-F88A to infect mouse, but not human, dendritic cells. Interestingly, however, not all mouse cells that permit GP-wt entry also permit GP-F88A entry. Among several mouse cell lines tested, including RAW 264.7 cells (Fig. 7A), GP-F88A VLPs successfully entered only the murine macrophage cell line IC-21 (Fig. 7B), demonstrating that the presence of mouse NPC1 is not sufficient for GP-F88A-mediated entry. Rather, NPC1 expression levels also appear to be important, as profiling of NPC1 mRNA levels demonstrated the highest levels in IC-21 and primary mouse PEMs (Fig. 7C). This is consistent with the observation that NPC1 overexpression in CHO cells gained permissiveness for GP-F88A-mediated entry (40). That a VSV pseudotyped with GP-F88A can initiate a replication cycle in IC-21 cells but not Vero cells indicates that the entry pathway(s) accessed by GP-F88A in these cells has relevance to virus infection (Fig. 7D). Cumulatively, the data in this study suggest that the affinity of GP_{CL} for NPC1, as well as the intracellular levels of NPC1, is an important determinant of EBOV entry into murine APCs. It will be of interest to determine whether cells that naturally express high levels of mouse NPC1 (e.g., IC-21 cells) or cells engineered to overexpress NPC1 will support the growth of recombinant filoviruses constructed with GP-F88A.

ACKNOWLEDGMENTS

This work is supported by NIH grants AI059536 and U54AI057158 (Northeast Biodefense Center-Lipkin) to C.F.B. and AI101436 to K.C.

REFERENCES

1. **Sanchez AG, Thomas W, Feldmann H.** 2007. Filoviridae: Marburg and Ebola Viruses. Lippincott Williams and Wilkins, Baltimore, MD.
2. **Borio L, Inglesby T, Peters CJ, Schmaljohn AL, Hughes JM, Jahrling PB, Ksiazek T, Johnson KM, Meyerhoff A, O'Toole T, Ascher MS, Bartlett J, Breman JG, Eitzen EM, Jr, Hamburg M, Hauer J, Henderson DA, Johnson RT, Kwik G, Layton M, Lillibridge S, Nabel GJ, Osterholm MT, Perl TM, Russell P, Tonat K.** 2002. Hemorrhagic fever viruses as biological weapons: medical and public health management. JAMA **287**: 2391–2405.
3. **Bray M, Davis K, Geisbert T, Schmaljohn C, Huggins J.** 1998. A mouse model for evaluation of prophylaxis and therapy of Ebola hemorrhagic fever. J. Infect. Dis. **178**:651–661.
4. **Connolly BM, Steele KE, Davis KJ, Geisbert TW, Kell WM, Jaax NK, Jahrling PB.** 1999. Pathogenesis of experimental Ebola virus infection in guinea pigs. J. Infect. Dis. **179**:S203–S217.
5. **Ebihara H, Takada A, Kobasa D, Jones S, Neumann G, Theriault S, Bray M, Feldmann H, Kawaoka Y.** 2006. Molecular determinants of Ebola virus virulence in mice. PLoS Pathog. **2**:e73. doi:10.1371/journal.ppat.0020073.
6. **Volchkov VE, Chepurnov AA, Volchkova VA, Ternovoj VA, Klenk HD.** 2000. Molecular characterization of guinea pig-adapted variants of Ebola virus. Virology **277**:147–155.
7. **Bray M.** 2001. The role of the type I interferon response in the resistance of mice to filovirus infection. J. Gen. Virol. **82**:1365–1373.
8. **Bar S, Takada A, Kawaoka Y, Alizon M.** 2006. Detection of cell-cell fusion mediated by Ebola virus glycoproteins. J. Virol. **80**:2815–2822.
9. **Neumann G, Geisbert TW, Ebihara H, Geisbert JB, Daddario-DiCaprio KM, Feldmann H, Kawaoka Y.** 2007. Proteolytic processing of the Ebola virus glycoprotein is not critical for Ebola virus replication in nonhuman primates. J. Virol. **81**:2995–2998.
10. **Neumann G, Feldmann H, Watanabe S, Lukashevich I, Kawaoka Y.** 2002. Reverse genetics demonstrates that proteolytic processing of the Ebola virus glycoprotein is not essential for replication in cell culture. J. Virol. **76**:406–410.
11. **Wool-Lewis RJ, Bates P.** 1999. Endoproteolytic processing of the ebola virus envelope glycoprotein: cleavage is not required for function. J. Virol. **73**:1419–1426.
12. **Volchkov VE, Feldmann H, Volchkova VA, Klenk HD.** 1998. Processing of the Ebola virus glycoprotein by the proprotein convertase furin. Proc. Natl. Acad. Sci. U. S. A. **95**:5762–5767.
13. **Kaletsky RL, Simmons G, Bates P.** 2007. Proteolysis of the Ebola virus glycoproteins enhances virus binding and infectivity. J. Virol. **81**:13378–13384.
14. **Kuhn JH, Radoshitzky SR, Guth AC, Warfield KL, Li W, Vincent MJ, Towner JS, Nichol ST, Bavari S, Choe H, Aman MJ, Farzan M.** 2006. Conserved receptor-binding domains of Lake Victoria marburgvirus and Zaire ebolavirus bind a common receptor. J. Biol. Chem. **281**:15951–15958.
15. **Lee JE, Saphire EO.** 2009. Ebolavirus glycoprotein structure and mechanism of entry. Future Virol. **4**:621–635.
16. **Dube D, Brecher MB, Delos SE, Rose SC, Park EW, Schornberg KL, Kuhn JH, White JM.** 2009. The primed ebolavirus glycoprotein (19-kilodalton GP1,2): sequence and residues critical for host cell binding. J. Virol. **83**:2883–2891.
17. **Ito H, Watanabe S, Sanchez A, Whitt MA, Kawaoka Y.** 1999. Mutational analysis of the putative fusion domain of Ebola virus glycoprotein. J. Virol. **73**:8907–8912.
18. **Weissenhorn W, Carfi A, Lee KH, Skehel JJ, Wiley DC.** 1998. Crystal structure of the Ebola virus membrane fusion subunit, GP2, from the envelope glycoprotein ectodomain. Mol. Cell **2**:605–616.
19. **Watanabe S, Takada A, Watanabe T, Ito H, Kida H, Kawaoka Y.** 2000. Functional importance of the coiled-coil of the Ebola virus glycoprotein. J. Virol. **74**:10194–10201.
20. **Hood CL, Abraham J, Boyington JC, Leung K, Kwong PD, Nabel GJ.** 2010. Biochemical and structural characterization of cathepsin L-processed Ebola virus glycoprotein: implications for viral entry and immunogenicity. J. Virol. **84**:2972–2982.

21. **Alvarez CP, Lasala F, Carrillo J, Muniz O, Corbi AL, Delgado R.** 2002. C-type lectins DC-SIGN and L-SIGN mediate cellular entry by Ebola virus in cis and in trans. J. Virol. **76**:6841–6844.
22. **Lin G, Simmons G, Pohlmann S, Baribaud F, Ni H, Leslie GJ, Haggarty BS, Bates P, Weissman D, Hoxie JA, Doms RW.** 2003. Differential N-linked glycosylation of human immunodeficiency virus and Ebola virus envelope glycoproteins modulates interactions with DC-SIGN and DC-SIGNR. J. Virol. **77**:1337–1346.
23. **Shimojima M, Takada A, Ebihara H, Neumann G, Fujioka K, Irimura T, Jones S, Feldmann H, Kawaoka Y.** 2006. Tyro3 family-mediated cell entry of Ebola and Marburg viruses. J. Virol. **80**:10109–10116.
24. **Takada A, Watanabe S, Ito H, Okazaki K, Kida H, Kawaoka Y.** 2000. Downregulation of [beta]1 integrins by Ebola virus glycoprotein: implication for virus entry. Virology **278**:20–26.
25. **Pipirou Z, Powlesland AS, Steffen I, Pohlmann S, Taylor ME, Drickamer K.** 2011. Mouse LSECtin as a model for a human Ebola virus receptor. Glycobiology **21**:806–812.
26. **Kondratowicz AS, Lennemann NJ, Sinn PL, Davey RA, Hunt CL, Moller-Tank S, Meyerholz DK, Rennert P, Mullins RF, Brindley M, Sandersfeld LM, Quinn K, Weller M, McCray PB, Jr, Chiorini J, Maury W.** 2011. T-cell immunoglobulin and mucin domain 1 (TIM-1) is a receptor for Zaire Ebolavirus and Lake Victoria Marburgvirus. Proc. Natl. Acad. Sci. U. S. A. **108**:8426–8431.
27. **Takada A, Fujioka K, Tsuiji M, Morikawa A, Higashi N, Ebihara H, Kobasa D, Feldmann H, Irimura T, Kawaoka Y.** 2004. Human macrophage C-type lectin specific for galactose and N-acetylgalactosamine promotes filovirus entry. J. Virol. **78**:2943–2947.
28. **Empig CJ, Goldsmith MA.** 2002. Association of the caveola vesicular system with cellular entry by filoviruses. J. Virol. **76**:5266–5270.
29. **Saeed MF, Kolokoltsov AA, Albrecht T, Davey RA.** 2010. Cellular entry of Ebola virus involves uptake by a macropinocytosis-like mechanism and subsequent trafficking through early and late endosomes. PLoS Pathog. **6**:e1001110. doi:10.1371/journal.ppat.1001110.
30. **Chandran K, Sullivan NJ, Felbor U, Whelan SP, Cunningham JM.** 2005. Endosomal proteolysis of the Ebola virus glycoprotein is necessary for infection. Science **308**:1643–1645.
31. **Bhattacharyya S, Warfield KL, Ruthel G, Bavari S, Aman MJ, Hope TJ.** 2010. Ebola virus uses clathrin-mediated endocytosis as an entry pathway. Virology **401**:18–28.
32. **Nanbo A, Imai M, Watanabe S, Noda T, Takahashi K, Neumann G, Halfmann P, Kawaoka Y.** 2010. Ebolavirus is internalized into host cells via macropinocytosis in a viral glycoprotein-dependent manner. PLoS Pathog. **6**:e1001121. doi:10.1371/journal.ppat.1001121.
33. **Aleksandrowicz P, Marzi A, Biedenkopf N, Beimforde N, Becker S, Hoenen T, Feldmann H, Schnittler HJ.** 2011. Ebola virus enters host cells by macropinocytosis and clathrin-mediated endocytosis. J. Infect. Dis. **204**(Suppl. 3):S957–S967.
34. **Mulherkar N, Raaben M, de la Torre JC, Whelan SP, Chandran K.** 2011. The Ebola virus glycoprotein mediates entry via a non-classical dynamin-dependent macropinocytic pathway. Virology **419**:72–83.
35. **Schornberg K, Matsuyama S, Kabsch K, Delos S, Bouton A, White J.** 2006. Role of endosomal cathepsins in entry mediated by the Ebola virus glycoprotein. J. Virol. **80**:4174–4178.
36. **Wong AC, Sandesara RG, Mulherkar N, Whelan SP, Chandran K.** 2010. A forward genetic strategy reveals destabilizing mutations in the Ebolavirus glycoprotein that alter its protease dependence during cell entry. J. Virol. **84**:163–175.
37. **Cote M, Misasi J, Ren T, Bruchez A, Lee K, Filone CM, Hensley L, Li Q, Ory D, Chandran K, Cunningham J.** 2011. Small molecule inhibitors reveal Niemann-Pick C1 is essential for Ebola virus infection. Nature **477**:344–348.
38. **Carette JE, Raaben M, Wong AC, Herbert AS, Obernosterer G, Mulherkar N, Kuehne AI, Kranzusch PJ, Griffin AM, Ruthel G, Dal Cin P, Dye JM, Whelan SP, Chandran K, Brummelkamp TR.** 2011. Ebola virus entry requires the cholesterol transporter Niemann-Pick C1. Nature **477**:340–343.
39. **Miller EH, Chandran K.** 2012. Filovirus entry into cells—new insights. Curr. Opin. Virol. **2**:206–214.
40. **Miller EH, Obernosterer G, Raaben M, Herbert AS, Deffieu MS, Krishnan A, Ndungo E, Sandesara RG, Carette JE, Kuehne AI, Ruthel G, Pfeffer SR, Dye JM, Whelan SP, Brummelkamp TR, Chandran K.** 2012. Ebola virus entry requires the host-programmed recognition of an intracellular receptor. EMBO J. **31**:1947–1960.
41. **Martinez O, Johnson J, Manicassamy B, Rong L, Olinger GG, Hensley LE, Basler CF.** 2010. Zaire Ebola virus entry into human dendritic cells is insensitive to cathepsin L inhibition. Cell Microbiol. **12**:148–157.
42. **Yonezawa A, Cavrois M, Greene WC.** 2005. Studies of Ebola virus glycoprotein-mediated entry and fusion by using pseudotyped human immunodeficiency virus type 1 virions: involvement of cytoskeletal proteins and enhancement by tumor necrosis factor alpha. J. Virol. **79**:918–926.
43. **Brindley MA, Hughes L, Ruiz A, McCray PB, Jr, Sanchez A, Sanders DA, Maury W.** 2007. Ebola virus glycoprotein 1: identification of residues important for binding and postbinding events. J. Virol. **81**:7702–7709.
44. **Martinez O, Valmas C, Basler CF.** 2007. Ebola virus-like particle-induced activation of NF-kappaB and Erk signaling in human dendritic cells requires the glycoprotein mucin domain. Virology **364**:342–354.
45. **Takada A, Robison C, Goto H, Sanchez A, Murti KG, Whitt MA, Kawaoka Y.** 1997. A system for functional analysis of Ebola virus glycoprotein. Proc. Natl. Acad. Sci. U S A **94**:14764–14769.
46. Reference deleted.
47. **Simmons G, Rennekamp AJ, Chai N, Vandenberghe LH, Riley JL, Bates P.** 2003. Folate receptor alpha and caveolae are not required for Ebola virus glycoprotein-mediated viral infection. J. Virol. **77**:13433–13438.
48. **Tscherne DM, Manicassamy B, Garcia-Sastre A.** 2010. An enzymatic virus-like particle assay for sensitive detection of virus entry. J. Virol. Methods **163**:336–343.
49. **Ou W, King H, Delisle J, Shi D, Wilson CA.** 2010. Phenylalanines at positions 88 and 159 of Ebolavirus envelope glycoprotein differentially impact envelope function. Virology **396**:135–142.
50. **Shah PP, Wang T, Kaletsky RL, Myers MC, Purvis JE, Jing H, Huryn DM, Greenbaum DC, Smith AB, III, Bates P, Diamond SL.** 2010. A small-molecule oxocarbazate inhibitor of human cathepsin L blocks severe acute respiratory syndrome and Ebola pseudotype virus infection into human embryonic kidney 293T cells. Mol. Pharmacol. **78**:319–324.
51. **Feldmann H, Volchkov VE, Volchkova VA, Klenk HD.** 1999. The glycoproteins of Marburg and Ebola virus and their potential roles in pathogenesis. Arch. Virol. Suppl. **15**:159–169.
52. **Geisbert TW, Hensley LE, Larsen T, Young HA, Reed DS, Geisbert JB, Scott DP, Kagan E, Jahrling PB, Davis KJ.** 2003. Pathogenesis of Ebola hemorrhagic fever in cynomolgus macaques: evidence that dendritic cells are early and sustained targets of infection. Am. J. Pathol. **163**:2347–2370.
53. **Lee JE, Fusco ML, Hessell AJ, Oswald WB, Burton DR, Saphire EO.** 2008. Structure of the Ebola virus glycoprotein bound to an antibody from a human survivor. Nature **454**:177–182.
54. **Mpanju OM, Towner JS, Dover JE, Nichol ST, Wilson CA.** 2006. Identification of two amino acid residues on Ebola virus glycoprotein 1 critical for cell entry. Virus Res. **121**:205–214.
55. **Bosio CM, Aman MJ, Grogan C, Hogan R, Ruthel G, Negley D, Mohamadzadeh M, Bavari S, Schmaljohn A.** 2003. Ebola and Marburg viruses replicate in monocyte-derived dendritic cells without inducing the production of cytokines and full maturation. J. Infect. Dis. **188**:1630–1638.
56. **Kash JC, Muhlberger E, Carter V, Grosch M, Perwitasari O, Proll SC, Thomas MJ, Weber F, Klenk HD, Katze MG.** 2006. Global suppression of the host antiviral response by Ebola- and Marburgviruses: increased antagonism of the type I interferon response is associated with enhanced virulence. J. Virol. **80**:3009–3020.
57. **Mercer J, Helenius A.** 2008. Vaccinia virus uses macropinocytosis and apoptotic mimicry to enter host cells. Science **320**:531–535.
58. **Bray M, Davis K, Geisbert T, Schmaljohn C, Huggins J.** 1999. A mouse model for evaluation of prophylaxis and therapy of Ebola hemorrhagic fever. J. Infect. Dis. **179**(Suppl. 1):S248–S258.
59. **Gupta M, Mahanty S, Ahmed R, Rollin PE.** 2001. Monocyte-derived human macrophages and peripheral blood mononuclear cells infected with Ebola virus secrete MIP-1alpha and TNF-alpha and inhibit poly-IC-induced IFN-alpha in vitro. Virology **284**:20–25.
60. **Hensley LE, Young HA, Jahrling PB, Geisbert TW.** 2002. Proinflammatory response during Ebola virus infection of primate models: possible involvement of the tumor necrosis factor receptor superfamily. Immunol. Lett. **80**:169–179.
61. **Bray M, Geisbert TW.** 2005. Ebola virus: the role of macrophages and dendritic cells in the pathogenesis of Ebola hemorrhagic fever. Int. J. Biochem. Cell Biol. **37**:1560–1566.
62. **Martinez O, Leung LW, Basler CF.** 2012. The role of antigen-presenting

cells in filoviral hemorrhagic fever: gaps in current knowledge. Antiviral Res. **93**:416–428.
63. **Manicassamy B, Wang J, Jiang H, Rong L.** 2005. Comprehensive analysis of ebola virus GP1 in viral entry. J. Virol. **79**:4793–4805.
64. **Marzi A, Akhavan A, Simmons G, Gramberg T, Hofmann H, Bates P, Lingappa VR, Pohlmann S.** 2006. The signal peptide of the ebolavirus glycoprotein influences interaction with the cellular lectins DC-SIGN and DC-SIGNR. J. Virol. **80**:6305–6317.
65. **Marzi A, Moller P, Hanna SL, Harrer T, Eisemann J, Steinkasserer A, Becker S, Baribaud F, Pohlmann S.** 2007. Analysis of the interaction of Ebola virus glycoprotein with DC-SIGN (dendritic cell-specific intercellular adhesion molecule-grabbing nonintegrin) and its homologue DC-SIGNR. J. Infect. Dis. **196**:S237–S246.
66. **Simmons G, Reeves JD, Grogan CC, Vandenberghe LH, Baribaud F, Whitbeck JC, Burke E, Buchmeier MJ, Soilleux EJ, Riley JL, Doms RW, Bates P, Pöhlmann S.** 2003. DC-SIGN and DC-SIGNR bind Ebola glycoproteins and enhance infection of macrophages and endothelial cells. Virology **305**:115–123.
67. **Baribaud F, Pohlmann S, Leslie G, Mortari F, Doms RW.** 2002. Quantitative expression and virus transmission analysis of DC-SIGN on monocyte-derived dendritic cells. J. Virol. **76**:9135–9142.
68. **Lasala F, Arce E, Otero JR, Rojo J, Delgado R.** 2003. Mannosyl glycodendritic structure inhibits DC-SIGN-mediated Ebola virus infection in cis and in trans. Antimicrob. Agents Chemother. **47**:3970–3972.
69. **Matsuno K, Nakayama E, Noyori O, Marzi A, Ebihara H, Irimura T, Feldmann H, Takada A.** 2010. C-type lectins do not act as functional receptors for filovirus entry into cells. Biochem. Biophys. Res. Commun. **403**:144–148.
70. **Gramberg T, Soilleux E, Fisch T, Lalor PF, Hofmann H, Wheeldon S, Cotterill A, Wegele A, Winkler T, Adams DH, Pohlmann S.** 2008. Interactions of LSECtin and DC-SIGN/DC-SIGNR with viral ligands: differential pH dependence, internalization and virion binding. Virology **373**:189–201.
71. **Powlesland AS, Fisch T, Taylor ME, Smith DF, Tissot B, Dell A, Pohlmann S, Drickamer K.** 2008. A novel mechanism for LSECtin binding to Ebola virus surface glycoprotein through truncated glycans. J. Biol. Chem. **283**:593–602.
72. **Dominguez-Soto A, Aragoneses-Fenoll L, Martin-Gayo E, Martinez-Prats L, Colmenares M, Naranjo-Gomez M, Borras FE, Munoz P, Zubiaur M, Toribio ML, Delgado R, Corbi AL.** 2007. The DC-SIGN-related lectin LSECtin mediates antigen capture and pathogen binding by human myeloid cells. Blood **109**:5337–5345.
73. **Gramberg T, Hofmann H, Moller P, Lalor PF, Marzi A, Geier M, Krumbiegel M, Winkler T, Kirchhoff F, Adams DH, Becker S, Munch J, Pohlmann S.** 2005. LSECtin interacts with filovirus glycoproteins and the spike protein of SARS coronavirus. Virology **340**:224–236.
74. **Sanchez A.** 2007. Analysis of filovirus entry into Vero E6 cells, using inhibitors of endocytosis, endosomal acidification, structural integrity, and cathepsin (B and L) activity. J. Infect. Dis. **196**:S251–S258.